PERGAMON

International Journal of Multiphase Flow 27 (2001) 2083–2103

International Journal of Multiphase Flow

www.elsevier.com/locate/ijmulflow

The motion of fibres in turbulent flow, stochastic simulation of isotropic homogeneous turbulence

James A. Olson

Department of Mechanical Engineering, Pulp and Paper Centre, The University of British Columbia, Vancouver, BC, Canada V6T 1Z4

Received 21 March 2000; received in revised form 9 July 2001

Abstract

The state of fibres suspended in a turbulent fluid is described in terms of a probability distribution function of fibre orientation and position throughout the suspending fluid. The evolution of the fibre's probability distribution function is governed by a convection–dispersion equation, where the randomizing effect of the turbulence is modelled by rotational and translational dispersion coefficients. To estimate these coefficients a numerical simulation of fibres moving in a turbulent fluid was developed. The trajectory of an ensemble of inertialess, rigid, thin, free-draining fibres was calculated through a stochastic model of homogeneous, isotropic turbulence. The results of the simulation were compared with analytical estimates and were found to provide reasonable agreement over a wide range of fibre length. However, the simulation showed that the Lagrangian integral time scale for rotation was significantly smaller than for translation and the ratio of rotational to translational Lagrangian time scales was smaller than the ratio of Eulerian time scales. The simulation also showed that the Lagrangian velocity correlation increased as fibre length increased and that the temporal correlations approached the analytical estimates of the Eulerian correlations in the limit of long fibres.

Keywords: Turbulence; Fibre; Suspension; Dispersion; Modelling; Pulp; Paper

1. Introduction

The behaviour of fibres in a turbulent flow affects the transport, rheology and light scattering properties of suspensions that are of interest in many areas of science and industry. Turbulent fibre suspensions are of particular interest in the pulp and paper industry, where nearly all fibre processing and papermaking is performed at high speeds in turbulent fluids. The complexity of turbulent fibre suspension has limited the application of advanced engineering techniques, for example computational fluid dynamics, to the design and optimization of the various unit operations and processes, resulting in lower product quality and productivity. Application of these

0301-9322/01/$ - see front matter
PII: S0301-9322(01)00050-7

techniques requires the development of a physical model of turbulent fibre suspension that can be implemented into predictive, computational tools.

The most common method of investigating fibre motion in flow is the Lagrangian approach, where the trajectory of individual fibres is determined by integrating the equations of motion through a known fluid velocity field. The other method is an Eulerian approach where fibre orientation and concentration distribution are calculated through the entire flow field simultaneously by considering the flux of particle centres and orientations. Although both approaches have separate strengths and are often complimentary, the Eulerian technique has several advantages, in that, it is more computationally efficient, naturally accounts for turbulent dispersion and most importantly has the potential to account for the interactions of the fibre on the fluid flow, i.e., can provide two-way coupling of the particle motion and flow.

In pulping and papermaking, fibre length is the most important property affecting the fibre's behaviour. Wood pulp suspension have a fibre length distribution that spans two orders of magnitude, from 0.05 to 5 mm, and for many applications, such as near wall flow or in the free jet of the forming section, fibre length is often larger than the turbulent length scale of the surrounding fluid. The effect of fibre length on the translation and orientation dispersion of fibres was first examined by Olson and Kerekes (1998). This theoretical study showed that both orientation and translational dispersion are reduced as fibre length increases due to averaging of eddy interactions along the fibre length. Although insightful, their study made a number of necessary, simplifying assumptions, for example, the Lagrangian statistics were assumed to be the same form as the Eulerian statistics, the longitudinal and transverse velocity correlations were made equivalent despite violating the continuity condition, and the Lagrangian integral time scales of fibre motion were assumed to be independent of fibre length. Clearly, these simplifications bring into question the application of analytic estimates of dispersion in predictive computational methods.

This work describes a numerical simulation of a single, thin, inertialess and rigid fibre moving in a stochastic turbulent velocity field described by the Kraichnan energy spectrum to study translational and rotational dispersion. The force on the fibre is modelled assuming a "free-draining" fibre and the motion of the fibre is calculated assuming a one-way coupling between the fibre and the fluid, i.e., the fibre does not influence the turbulent fluid. The simulation overcomes some of the shortcomings of the analytic expressions for dispersion mentioned previously, although is not without its own limitations. The results of the simulation are then compared with and interpreted in terms of the analytical expressions for dispersion derived by Olson and Kerekes (1998).

2. Background

Fibres in a turbulent fluid undergo mean and random motion and that motion is a combination of translation and rotation. In an Eulerian description of a fibre suspension, the position $\boldsymbol{r}$ and orientation $\boldsymbol{p}$ of the fibers at time t is denoted by a probability distribution function $\Psi(\boldsymbol{r},\boldsymbol{p},t)$. The evolution of Ψ is given by the following convection–dispersion equation

$$\frac{\partial \Psi}{\partial t} = D_{\mathrm{r}}\nabla_{\mathrm{r}}^2\Psi - \nabla_{\mathrm{r}}\cdot(\boldsymbol{\Omega}\Psi) + D_{\mathrm{t}}\nabla^2\Psi - \nabla\cdot(\boldsymbol{V}\Psi), \tag{1}$$

where the terms on the right-hand side are the rotational dispersion, mean rotation, translational dispersion and mean translation, respectively Doi and Chen, 1989. Here, ∇_r is the rotational operator, similar to the angular momentum operator in quantum mechanics, and is expressed as

$$\nabla_r = \boldsymbol{p} \times \frac{\partial}{\partial \boldsymbol{p}}. \tag{2}$$

The fibre's angular velocity, $\boldsymbol{\Omega}$, is related to the fibres rotational vector by the following:

$$\boldsymbol{\Omega} = \boldsymbol{p} \times \dot{\boldsymbol{p}}. \tag{3}$$

To apply Eq. (1), expressions need to be developed that link the rotational dispersion coefficient, D_r, and the translational dispersion coefficient, D_t to the properties of the turbulence. Olson and Kerekes (1998) derived the following approximate expressions for the translational and rotational dispersion coefficients assuming a free-draining, inertialess, rigid fibre of length L moving in a homogeneous, isotropic turbulent fluid,

$$D_t = \frac{2\langle u^2 \rangle}{L^2} \frac{d}{dt} \int_0^t \int_0^L (t-\tau)(L-l)\mathscr{R}(l,\tau)\, dl\, d\tau \tag{4}$$

and

$$D_r = \frac{24\langle u^2 \rangle}{L^3} \frac{d}{dt} \int_0^t \int_0^L (t-\tau)\left(1 - 3\frac{l}{L} + 2\left(\frac{l}{L}\right)^3\right)\mathscr{R}(l,\tau)\, dl\, d\tau, \tag{5}$$

where $\mathscr{R}(l,\tau)$ is the Lagrangian fibre velocity correlation and $\langle u^2 \rangle$ is the turbulent intensity. In the analysis of Olson and Kerekes, $\mathscr{R}(l,\tau)$ was approximated as the product of the fluids Eulerian spatial velocity correlation and the Lagrangian velocity correlation of the fluid. The velocity correlation of the fibre was shown to equal the the Lagrangian velocity correlation of the fluid for short fibres and was hypothesized to be equal to the Eulerian velocity correlation of the fluid for infinitely long fibres.

In this study, a numerical simulation of individual fibres moving in a random velocity field is used to develop approximate relations between the Lagrangian fibre correlations required by the translational and rotational dispersion coefficients, Eqs. (4) and (5), and a specified Eulerian fluid velocity correlations. Specifically, the Eulerian fluid correlations correspond to the Kraichnan energy spectrum and are not general to other spectra, however, the approach is general and could be applied to other model spectra.

3. Numerical simulation

In this section, the equations of motion for a rigid, infinitely thin fibre of arbitrary length are derived, as well, the model for the turbulent velocity field is described. These two models are then combined in a "one-way coupling" (McLaughlin, 1994), such that the fibre is assumed not to significantly affect the turbulent velocity field. Of course, real fibre suspensions can significantly affect the turbulent velocity field, especially at high concentrations where it is expected that the small scales of turbulence would be quickly dissipated. Therefore, this simplification assumes a dilute fibre suspension. Modelling the suspension using "two-way coupling" is complex and has

not been completely successfully. The complexity of the interactions between the particles and the fluid turbulence is illustrated in the experimental studies performed by Gore and Crowe (1989).

Fibre trajectory is calculated using the standard ODEPACK routines for ordinary differential equations (INRIA, 1999). These routine automatically select between the non-stiff predictor–corrector Adams method and stiff backward differentiation formula (BDF) method. It uses the non-stiff method initially and dynamically monitors data in order to decide which method to use. The simulation calculates a relatively large number of individual fibre trajectories, typically 1000, from which the necessary Lagrangian statistics are gathered.

3.1. Fibre motion

The derivation of the equations of fibre motion in a turbulent flow requires a model of the force imposed on the fibre by the fluid. Unfortunately, there is no slender body theory that is strictly valid for the high Reynold's number, turbulent flow of interest here. As a necessary simplification, the form of the force on the fibre under creeping flow conditions, derived by Cox (1970) given by Eq. (6), is assumed to be retained for higher Reynold's number flows

$$\boldsymbol{f}\ (l) = D[\boldsymbol{u}(l) - \boldsymbol{v}(l)]. \tag{6}$$

For straight rigid infinitely thin fibres D is independent of position along the fibre, l, and is given by

$$D = \frac{4\pi\mu[\boldsymbol{pp} - 2\boldsymbol{I}]}{\ln\kappa}, \tag{7}$$

where κ is the aspect ratio of the fibres (assumed to be large). However, Eq. (6) was derived for a small Reynold's number flow where Reynold's number is based on fibre length, L. Therefore, Eq. (6) is only strictly valid for infinitely thin fibres with L less than the Kolmogorov length scale, η, of the turbulence. Eq. (6) is applied to longer fibres suspended in turbulent flow, by imposing the free-draining approximation used to model flexible fibre motion (Ross and Klingenberg, 1997), and to model polymer dynamics (Doi and Chen, 1989; Doi and Edwards, 1988). Hence, the fibre is considered to be composed of a series of elements Δ_l long, where $\Delta_l < \eta$, and each element is assumed to be hydrodynamically independent. In this model of a fibre, each element meets the necessary conditions for Eq. (6) to be valid, and assuming hydrodynamic independence of each element allows Eq. (6) to be applied to all elements, thus applied to the entire fibre. The lack of an accurate model of force on a long fibre in high Reynolds number flow ($Re > 1$) and the necessity of imposing the free-draining approximation limits the quantitative predictability of Eq. (6) for long fibres. The results have to be interpreted in light of this and other approximations made in this paper.

Assuming a straight rigid fibre, the velocity at any point along the fibre will be the sum of the fibres translational velocity, $\boldsymbol{v}$, and rotational velocity, $l\dot{\boldsymbol{p}}$, where $\dot{\boldsymbol{p}}$ is the time derivative of a unit vector parallel to the fibre's major axis, and l is the distance from the fibre centre (see Fig. 1). The net external force, $\boldsymbol{F}$, on the particle is obtained by integrating Eq. (6) along the length of the fibre, given by

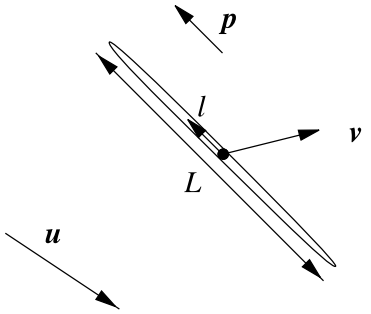

Fig. 1. A straight rigid fibre of length L, moving with velocity $\boldsymbol{v}$, in a turbulent fluid with velocity $\boldsymbol{u}$. The fibre is pointing in the direction given by unit vector $\boldsymbol{p}$.

$$\boldsymbol{F} = \int_{-L/2}^{L/2} D[\boldsymbol{u}(l) - (\boldsymbol{v} + l\dot{\boldsymbol{p}})]\,\mathrm{d}l. \tag{8}$$

The net external moment acting on the fibre is similarly given by

$$\boldsymbol{M} = \int_{-L/2}^{L/2} l\boldsymbol{p}_f \times D[\boldsymbol{u}(l) - (\boldsymbol{v} + l\dot{\boldsymbol{p}})]\,\mathrm{d}l. \tag{9}$$

Assuming the fibre is neutrally buoyant, and inertial forces are negligible in generating relative velocities between the particle and fluid results in $\boldsymbol{F} = 0$ and $\boldsymbol{M} = 0$. For this condition,

$$\boldsymbol{v} = \frac{1}{L}\int_{-L/2}^{L/2} \boldsymbol{u}(\boldsymbol{y} + l\boldsymbol{p}, t)\,\mathrm{d}l \tag{10}$$

and

$$\boldsymbol{\Omega} = \boldsymbol{p} \times \frac{12}{L^3}\int_{-L/2}^{L/2} l\boldsymbol{u}(\boldsymbol{y} + l\boldsymbol{p}, t)\,\mathrm{d}l, \tag{11}$$

where $\boldsymbol{\Omega}$ is the angular velocity of the fibre. The equations for the mean velocity required in Eq. (1) are also given by Eqs. (10) and (11), if the mean fluid velocity is substituted for $\boldsymbol{u}$. The rate of change of orientation, $\dot{\boldsymbol{p}}$, is then calculated as

$$\dot{\boldsymbol{p}} = \boldsymbol{\Omega} \times \boldsymbol{p}. \tag{12}$$

Eqs. (10)–(12) can be numerically integrated to provide the trajectory of the fibre through the fluid. These equations for fibre motion have been used to model a fibre moving in non-homogeneous flow, i.e., non-linear shear, by several investigators: Riese et al. (1969), Shanker et al. (1991), Pittman and Kasiri (1992), Tangsaghasaksri (1994) and Olson (1996).

To simplify the calculation, the orientation is expressed in terms of its orientation angles, θ and ϕ, where

$$\boldsymbol{p} = \begin{bmatrix} \cos\phi\sin\theta \\ \sin\phi\sin\theta \\ \cos\theta \end{bmatrix} \tag{13}$$

with corresponding unit vectors given by

$$\hat{\boldsymbol{\theta}} = \begin{bmatrix} \cos\phi\cos\theta \\ \sin\phi\cos\theta \\ -\sin\theta \end{bmatrix} \quad \text{and} \quad \hat{\boldsymbol{\phi}} = \begin{bmatrix} -\sin\phi \\ \cos\phi \\ 0 \end{bmatrix}.$$

The orientational velocity is then

$$\dot{\boldsymbol{p}} = \dot{\phi}\sin\theta\hat{\boldsymbol{\phi}} + \dot{\theta}\hat{\boldsymbol{\theta}}. \tag{14}$$

The angular velocity of the fibre is given by the following differential equations:

$$\dot{\phi} = \frac{12}{L^3\sin\theta}\int_{-L/2}^{L/2} l\hat{\boldsymbol{\phi}}\cdot\boldsymbol{u}(\boldsymbol{y}+l\boldsymbol{p},t)\,\mathrm{d}l, \tag{15}$$

and

$$\dot{\theta} = \frac{12}{L^3}\int_{-L/2}^{L/2} l\hat{\boldsymbol{\theta}}\cdot\boldsymbol{u}(\boldsymbol{y}+l\boldsymbol{p},t)\mathrm{d}l. \tag{16}$$

In this study Eqs. (10), (15) and (16) are numerically integrated through a specified fluid velocity field, $\boldsymbol{u}(\boldsymbol{x},t)$, to determine the fibre's trajectory.

3.2. Turbulent velocity field

The turbulent fluid velocity, $\boldsymbol{u}(\boldsymbol{x},t)$, has been modelled by many investigators studying particle dispersion as a stochastic series of independent Fourier modes. Following these researches $\boldsymbol{u}(\boldsymbol{x},t)$ is given as

$$\boldsymbol{u}(\boldsymbol{x},t) = \sum_{n=1}^{N} \boldsymbol{A}^{(n)}\sin(\boldsymbol{k}^{(n)}\boldsymbol{x}+\omega^{(n)}t) + \boldsymbol{B}^{(n)}\cos(\boldsymbol{k}^{(n)}\boldsymbol{x}+\omega^{(n)}t). \tag{17}$$

The coefficients $A_i^{(n)}$ and $B_i^{(n)}$ are random velocity given by

$$\boldsymbol{A}^{(n)} = \boldsymbol{\xi}^{(n)} \times \frac{\boldsymbol{k}^{(n)}}{|\boldsymbol{k}^{(n)}|}, \tag{18}$$

and

$$\boldsymbol{B}^{(n)} = \boldsymbol{\zeta}^{(n)} \times \frac{\boldsymbol{k}^{(n)}}{|\boldsymbol{k}^{(n)}|}, \tag{19}$$

to ensure incompressibility

$$\nabla\cdot\boldsymbol{u}(\boldsymbol{x},t) = 0. \tag{20}$$

The components of each random coefficients $\xi_i^{(n)}$ and $\zeta_i^{(n)}$ are chosen from a Gaussian random distribution with zero mean and standard deviation $3u_0/(2N)^{1/2}$.

Each wave vector $\boldsymbol{k}^{(n)}$ is chosen to be uniformly distributed over the surface of a sphere of radius $k^{(n)}$

$$\int_0^{k^{(n)}} E(k)\,\mathrm{d}k = \frac{3(n-1/2)u_0^2}{2N}, \tag{21}$$

where

$$E(k) = 16(2/\pi)^{1/2}\frac{u_0^2 k^4}{k_0^5}\exp(-2(k/k_0)^2). \tag{22}$$

This ensures that the resulting energy spectrum is the Kraichnan energy spectrum, which is representative of low Reynolds number turbulence behind a grid (Hinze, 1975). The energy spectrum is a maximum at $k = k_0$. The corresponding longitudinal and transverse velocity correlations are given by

$$f(r) = \exp\left(-\frac{r^2k_0^2}{8}\right), \tag{23}$$

$$g(r) = \left(1-\frac{r^2k_0^2}{8}\right)\exp\left(-\frac{r^2k_0^2}{8}\right). \tag{24}$$

To model higher Reynolds number turbulence others have used the same approach with different energy spectra, for example, the von Kármán–Pao spectrum (Wang and Stock, 1994).

The frequencies $\omega^{(n)}$ are also chosen from a Gaussian distribution with zero mean and standard deviation $\omega_0 = au_0k^{(n)}$, where u_0 is the rms velocity of the fluctuating component of the fluid velocity. The resulting energy spectrum is given by

$$\mathscr{E}(k,\omega) = E(k)\exp\left(-\frac{\omega^2}{2(aku_0)^2}\right)\Big/((2\pi)^{1/2}aku_0), \tag{25}$$

which shows good agreement with the direct numerical simulation of Hunt et al. (1987) for $a = 0.40$.

This stochastic approach to modelling isotropic homogeneous turbulence has been used by several investigators to study particle dispersion because of its ability to reproduce the required two-point Eulerian statistics while predicting many features of the Lagrangian statistics. Kraichnan (1970) was the first to use this technique as a statistical test of the direct-interaction approximation of turbulent self-diffusion. Maxey (1987) used Kraichnan's method to study the settling velocity of small spherical particles with and without inertia. Here, each wave vector component was independently chosen from a Gaussian distribution and the temporal frequencies were chosen from an independent Gaussian distribution with a characteristic frequency ω_0 that was independent of $k^{(n)}$. They modelled the force imposed on the particle by the fluid, assuming a Stokes drag and examined particle dispersion for varying ω_0. Maxey also points out some of the shortcoming of this stochastic model of turbulence: there is no representation of the energy transfer between large and small eddies, no advection of small eddies by larger eddies and the triple correlations of velocity vanish. This brings into question the quantitative prediction of this model, however, the qualitative predictions and insight have been valuable in many of the following studies.

Wang and Stock (1992) used the same model as Maxey to examine the effect of non-linear drag on the dispersion of small particles. In another study, Wang and Stock (1994) modified the

turbulence model to account for the effect of turbulence decay in the wake of a grid by incorporating time varying u_0 and ω_0. These studies used both the Kraichnan energy spectrum to model low Reynolds number turbulence and the von Kármán–Pao energy spectrum to model higher Reynolds number turbulence. Furthermore, both turbulence models were shown to provide excellent agreement with the experimental measurements of particle dispersion in grid-generated turbulence performed by Snyder and Lumley (1971). Similarly, Mei (1994) used this technique to examine the effect of non-linear drag on particle settling time. Spelt and Biesheuvel (1997) used the same model of turbulence as this study to examine the motion of small bubbles in isotropic turbulence.

Fung et al. (1992) further modified the turbulence model to account for the advection of small eddies by larger eddies and used this model to study the relations between the Eulerian and Lagrangian structures of turbulence. In addition, they provide a good discussion of the applicability of these models to true flows based on dimensional scaling arguments. Fung et al. point out that the advection of small eddies by larger eddies can also be accounted for by coupling this approach with techniques such as large-eddy simulation. In a subsequent study, Fung (1993) used this extended turbulence model to predict the gravitational settling of small particles (Fung, 1993).

Recently, Newson and Bruce (1998) used a similar stochastic representation of turbulence to model the orientation of small fibres settling in atmospheric turbulence. The results of the simulation were compared to experimental measurements of mean orientation determined using millimeter wave depolarization techniques. Unfortunately, this study only looked at the mean orientation of the fibres during settling and did not consider the general problem of fibre dispersion of interest to this study.

4. Results

For each fibre length, k_0L equal to 0.25, 1.0, 3, 5, 7, 10 and 20, 1000 trajectories were calculated, each through a newly generated realization of the random flow field. For all simulations the number of Fourier modes, N, was equal to 100. From the ensemble of fibre trajectories the required fibre and fluid velocity correlations were calculated.

The turbulent fluid velocity is defined by setting two parameters: $k_0 = 1.0$ and $u_0 = 1.0$. Assuming the von Kármán energy spectrum, the maximum energy containing wave vector corresponds to $k = k_0$ and the range of length scales is approximately $0.25 < k/k_0 < 2$. The corresponding Kolmogorov scale for such turbulence is approximately given by $(2k_0)^{-1}$. Furthermore, all the analyses presented in this section are made by assuming that the turbulence is well represented by a von Kármán spectrum.

4.1. Fluid statistics

The Eulerian longitudinal and transverse fluid velocity correlations were calculated from the numerical simulation and are given in Fig. 2 and compared with the exact correlations given by Eqs. (23) and (24). The results of averaging over 1000 realization compares well with the analytic solution and demonstrates the ability and accuracy of the numerical method to converge to the exact Eulerian correlations.

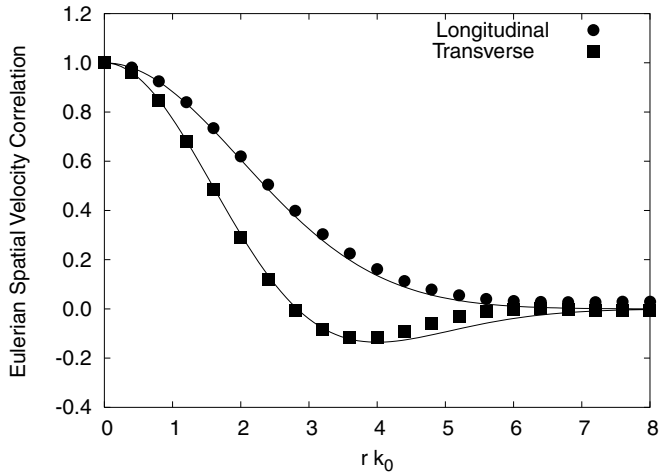

Fig. 2. The Eulerian transverse and longitudinal velocity correlation of the fluid model as determined by the simulation (points) and the exact correlations (lines).

In Fig. 3, the Eulerian temporal velocity correlation was also calculated and compared to the exact solution given by

$$\frac{\langle \boldsymbol{u}(0)\boldsymbol{u}(\tau)\rangle}{\boldsymbol{u}^2} = \frac{32}{(4+\omega_0^2\tau^2)^{5/2}}, \tag{26}$$

where the average Eulerian frequency is given by $\omega_0 = ak_0u_0$.

The Lagrangian fluid velocity correlation was similarly determined by calculating the trajectory of fluid elements through the turbulent velocity field by directly integrating Eq. (17). The Lagrangian temporal correlation was then compared to Eq. (26) for a best-fit value of $\omega_0 = 1.0$

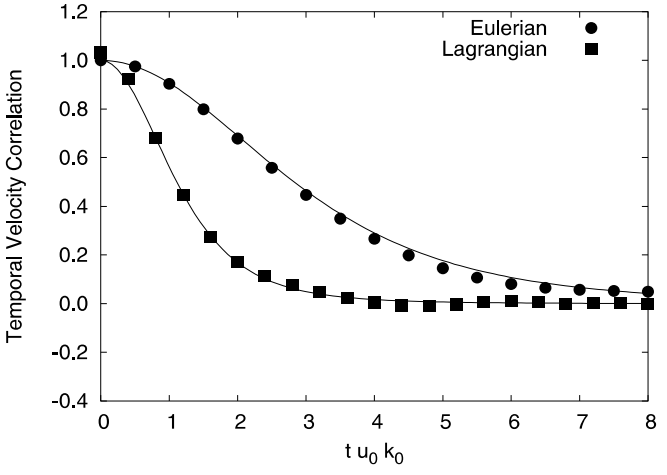

Fig. 3. The Eulerian and Lagrangian temporal velocity correlation of the fluid as determined by the simulation (points) and the exact expression for the Eulerian velocity (line).

in Fig. 3. For this turbulence model, the form of the Lagrangian velocity correlation is similar to the form of the Eulerian correlation, with the ratio of Eulerian to Lagrangian values of ω_0 approximately equal to 0.4.

4.2. Fibre statistics

4.2.1. Translational dispersion

All fibre trajectories have initial conditions of $\boldsymbol{p} = \hat{1}$, $\boldsymbol{y} = 0$ at $t = 0$. The fibre translation is given by integrating Eq. (10), i.e.

$$\boldsymbol{y}(t) = \int_0^t \boldsymbol{v}(\tau)\, \mathrm{d}\tau. \tag{27}$$

The mean square translation of the fibres, $\langle \boldsymbol{y}^2 \rangle$ as a function of time is given in Fig. 4 for all fibre lengths. The fibres initially disperse slowly corresponding to the velocity being initially strongly correlated with time, and after several eddy interactions disperse linearly with time. This trend is similar for all fibre lengths examined. Fibres shorter than the smallest scales of turbulence disperse at the same rate as the fluid particles, which corresponds with the assumption of an inertialess fibre. As fibre length increases the rate of translational dispersion decreases. The decrease in dispersion is due to a decreased magnitude of fibre velocity fluctuations caused by averaging of the turbulent fluctuations over the length of the fibre.

The translational dispersion coefficient that characterizes turbulent motion in Eq. (1) is calculated from the mean square translation of fibres originating from a point source (Hinze, 1975) from the following relation:

$$D_\mathrm{t} = \frac{1}{6} \frac{\mathrm{d}\langle \boldsymbol{y}^2 \rangle}{\mathrm{d}t}. \tag{28}$$

The translational dispersion coefficient was calculated for all fibre lengths from the mean square translation using Eq. (28) and plotted in Fig. 5. As expected the dispersion coefficient is initially

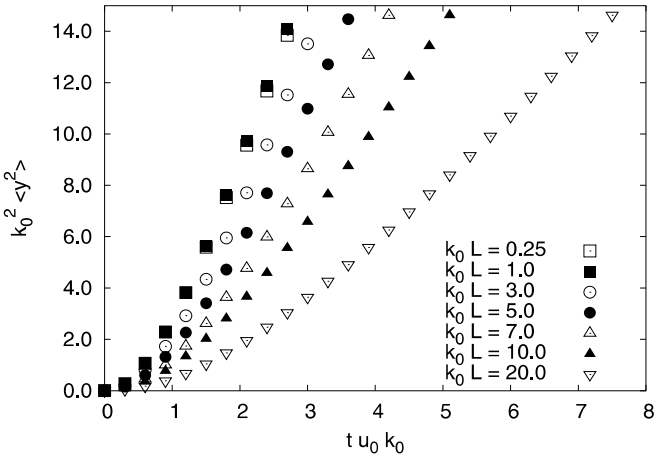

Fig. 4. The mean square translation of fibres, $\langle \boldsymbol{y}^2 \rangle$.

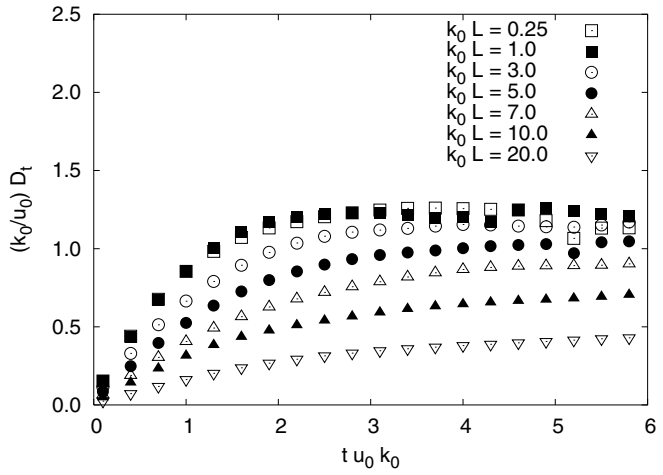

Fig. 5. Translational dispersion coefficient.

zero and increases quickly to a constant value, D_t^∞, the long-time, translational dispersion coefficient. The time it takes to reach this steady-state value corresponds to the time required for the translation to be uncorrelated and is therefore approximately equal to twice the Lagrangian integral time scale, which is approximately $t > 2.5/u_0k_0$ for shorter fibres. The dispersion coefficient of the smallest fibres ($k_0L \leqslant 1.0$), which undergo the largest amount of dispersion, have the largest error in the calculation due to the finite number of trajectories calculated, especially when taking the derivative of the correlation. However, within error the dispersion coefficient is approximately constant, as expected, and a good estimate of D_t^∞ can be made. For the longest fibres, the dispersion coefficient is still slowly increasing and does not reach its constant value until later times.

Of most interest to the application of numerical simulations of turbulent fibre suspensions is the long-time dispersion coefficient, D_t^∞, which is estimated from the asymptotic value of the

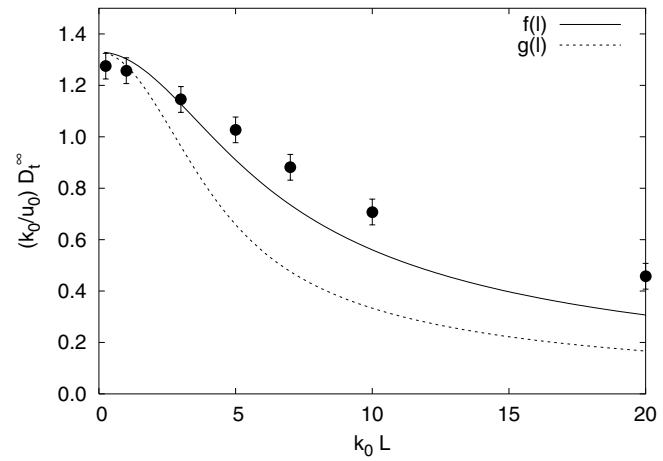

Fig. 6. Long-time translational dispersion coefficient.

calculated D_t shown in Fig. 5. The calculated values of D_t^∞ are given in Fig. 6. Here again, the decreasing dispersion with increasing fibre length is evident.

The analytic estimate of D_t^∞ derived by Olson and Kerekes (1998), who assumed that the spatial statistics of the fibre velocity correlation are independent of the temporal statistics, is given by the following:

$$D_t^\infty = \frac{2u^2}{L^2} T_t \int_0^L (L-l)\mathscr{R}(l)\,\mathrm{d}l, \tag{29}$$

where T_t is the integral time scale of the Lagrangian fibre velocity correlation. For short fibres, i.e., $L = 0, T$ equals the integral time scale of Lagrangian fluid velocity correlation and it was hypothesized that for long fibres, i.e., $L \to \infty$, T_t equals the Eulerian fluid velocity correlation. To calculate D_t^∞, Olson and Kerekes (1998) approximated T_t by the integral time scale of the fluids Lagrangian velocity correlation and approximated $\mathscr{R}(l)$ by the Eulerian longitudinal and lateral velocity correlations, $f(l)$ and $g(l)$. The fibres spatial velocity correlation, $\mathscr{R}(l)$ is expected to be bracketed by the two correlations $f(l)$ and $g(l)$, since translation may be due to fluid velocity in the direction of, or perpendicular to the direction of the fibre, depending on fibre orientation. The value of D_t^∞ estimated from the simulation and calculated from Eq. (29) is given in Fig. 6. From Fig. 6 it is evident that Eq. (29) underestimates the simulated dispersion coefficient for both approximations of the spatial correlations $f(l)$ and $g(l)$ if a constant integral time scale is assumed.

To examine the effect of fibre length on the integral time scale, the fibre's temporal velocity correlation is estimated from the simulation and plotted in Fig. 7. The fibre's temporal velocity correlation is defined as $\langle \boldsymbol{v}(0)\boldsymbol{v}(t)\rangle / \langle \boldsymbol{v}^2 \rangle$. The solid lines are the fluid's Lagrangian and Eulerian velocity correlations. As hypothesized, the fibres Lagrangian velocity correlations initially equals the fluids Lagrangian correlation for the shortest fibres ($L \to 0$) and approaches the Eulerian velocity correlation as fibre length increases.

From the velocity correlation, the integral time scale is estimated by numerically determining the best-fit value of ω_0 to Eq. (26) and then integrating Eq. (26) to calculate T_t. This necessarily

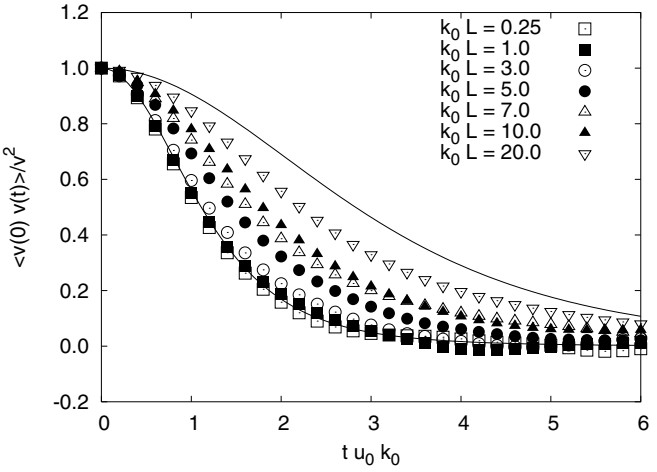

Fig. 7. The translational velocity correlation.

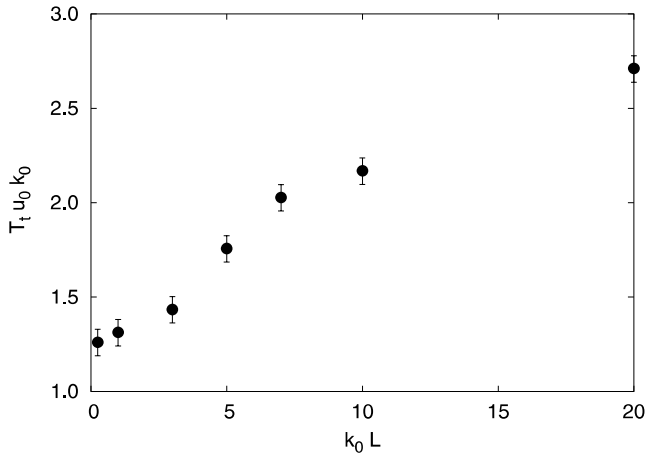

Fig. 8. The fibre Lagrangian integral time scale.

assumes that Eq. (26) provides the proper form for the Lagrangian statistics, which turns out to be a good approximation. The integral time scale for each fibre length is plotted in Fig. 8. The increase in integral time scale with increasing fibre length is approximately linear initially and asymptotically approaches the Eulerian integral time scale as fibre length becomes large. Note that the fluids Eulerian integral time scale is equal to $4/3(0.4)k_0u_0 = 3.33k_0u_0$ and the fluids Lagrangian integral time scale is determined to be approximately $1.31k_0u_0$. To accurately model the length dependence on dispersion the effect of increasing Lagrangian integral time scale with fibre length must be taken into account.

The increase in fibre Lagrangian time scale from the fluids Lagrangian time scale to the Eulerian time scale as fibre length increases is similar to that observed and predicted for heavy particles in turbulent flow. The increase in integral time scale for increasing inertia is sometimes referred to as the the crossing-trajectory effect (Reeks, 1977; Pismen and Nir, 1978). As inertia increases the particle experiences near-Eulerian velocity statistics as the particle's translation becomes less effected by the fluid's fluctuating velocity.

4.2.2. Rotational dispersion

From the ensemble of fibre trajectories, the orientation correlation is calculated as $\langle \boldsymbol{p}(0)\boldsymbol{p}(t)\rangle / \langle \boldsymbol{p}^2\rangle$ and given in Fig. 9 for all fibre lengths. From this figure, it is evident that short fibres are completely randomized after approximately $4/k_0u_0$ and that longer fibres require more time to disperse, with the longest fibres remaining strongly correlated beyond $8/u_0k_0$. The decrease in dispersion with increasing fibre length is due to the decrease in angular velocity fluctuations caused by averaging fluid fluctuations along the length of the fibre and is similar to the observed decrease in translational dispersion.

The rotational dispersion coefficient that characterizes the turbulent rotation in Eq. (1) is calculated from the mean rotational dispersion using the following relation (See Appendix A):

$$D_r = -\frac{\partial\langle \boldsymbol{p}(0)\boldsymbol{p}(t)\rangle}{\partial t} \Big/ (2\langle \boldsymbol{p}(0)\boldsymbol{p}(t)\rangle). \tag{30}$$

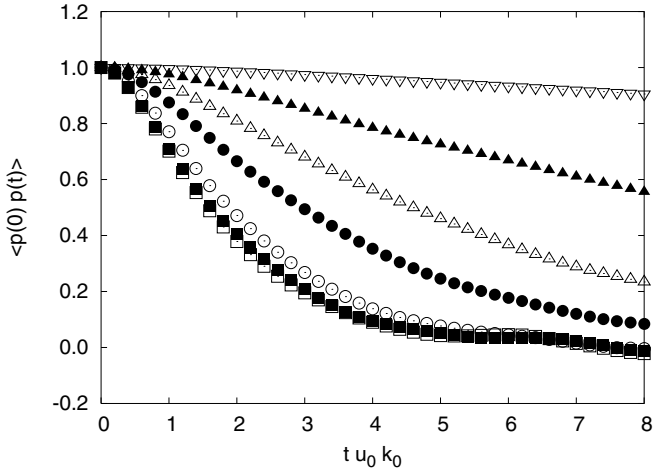

Fig. 9. The mean square fibre orientation.

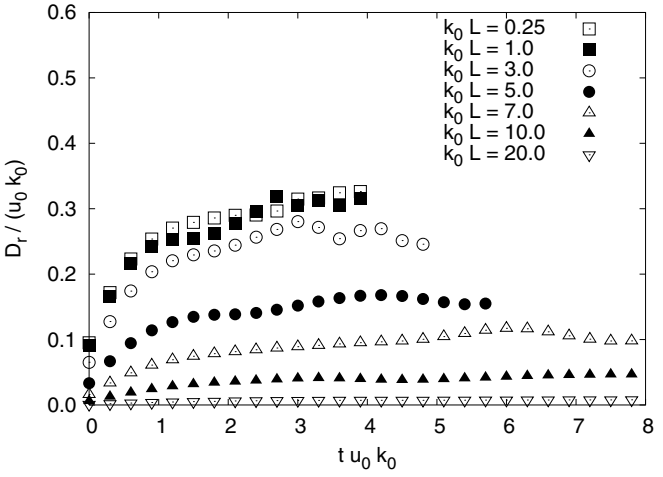

Fig. 10. The rotational dispersion coefficient for all fibre lengths.

The rotational dispersion coefficient is plotted as a function of time in Fig. 10. As with translational dispersion, the rotational dispersion coefficient is initially zero and increases until it reaches a maximum value, where after it remains constant. This constant value is the long-time rotational dispersion coefficient, denoted by D_r^{∞}. The value of D_r^{∞} is calculated from the asymptotic value of D_r and is plotted in Fig. 11. The figure demonstrates the strong dependence of fibre length on rotational dispersion.

Accurately determining D_r^{∞} from Eq. (30) is difficult because the fibre orientation correlation is nearly zero for short fibres before the dispersion coefficient reaches a constant value, therefore estimates of D_r^{∞} are made from relatively noisy statistics. The reported error-bars represent 95% confidence limits, estimated from the variance of D_r near the region of constant value.

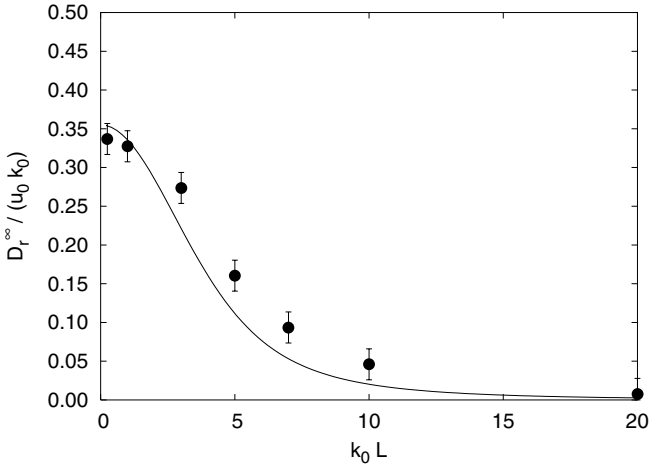

Fig. 11. The long-time rotational dispersion coefficient.

The approximate analytical expression for D_r^∞ derived by Olson and Kerekes (1998) is given by

$$D_r^\infty = \frac{24u_0^2 T_r}{L^3} \int_0^L \left(1 - \frac{3l}{L} + 2\left(\frac{l}{L}\right)^3\right) \mathscr{R}(l)\, dl. \tag{31}$$

To relate this expression to the available Eulerian statistics, the correlation $\mathscr{R}(l)$ was approximated as the Eulerian lateral velocity correlation, $g(l)$, since rotation is due entirely to the component of fluid velocity perpendicular to the fibre. This approximation also assumes the turbulence is ergodic in the sense that integrating along the length of an ensemble of fibres is equivalent to integrating along an arbitrary line in the flow. The relevant integral time scale T_r, is the integral time scale of the angular velocity

$$T_r = \int_0^\infty \frac{\langle \boldsymbol{\Omega}(0)\boldsymbol{\Omega}(\tau)\rangle}{\langle \boldsymbol{\Omega}^2\rangle}\, d\tau, \tag{32}$$

where $\boldsymbol{\Omega} = \boldsymbol{p} \times \dot{\boldsymbol{p}}$.

Before calculating T_r and subsequently D_r^∞, it is necessary to discuss the angular velocity correlation in some detail. First, an analytic approximation of the the Eulerian angular velocity correlation is derived, where Eulerian refers to short fibres that do not rotate significantly before the angular velocity becomes uncorrelated. This is analogous to interpreting the Eulerian velocity correlation as the velocity correlation of a particle that does not move significantly. The form of the Eulerian correlation is then used to approximate the form of the Lagrangian correlation, as was done previously with the translational velocity correlations.

Assuming $\dot{\boldsymbol{p}}$ is small, such that $\boldsymbol{p}$ is does not change significantly over the integral time scale, then

$$\frac{\langle \boldsymbol{\Omega}(0)\boldsymbol{\Omega}(\tau)\rangle}{\langle \boldsymbol{\Omega}^2\rangle} \approx \frac{\langle \dot{\boldsymbol{p}}(0)\dot{\boldsymbol{p}}(\tau)\rangle}{\langle \dot{\boldsymbol{p}}^2\rangle}. \tag{33}$$

Now, without loss of generality, consider a fibre oriented in the y_1 direction, then for short fibres

$$\dot{p}_1 = \frac{\partial u_1}{\partial y_2}, \tag{34}$$

thus

$$\frac{\langle \dot{p}_1(0)\dot{p}_1(\tau)\rangle}{\langle \dot{p}_1^2\rangle} = \left\langle \frac{\partial u_1(0)}{\partial y_2}\frac{\partial u_1(\tau)}{\partial y_2}\right\rangle \Big/ \left\langle \left(\frac{\partial u_1}{\partial y_2}\right)^2\right\rangle = \frac{\partial^2 g(l,\tau)}{\partial l^2}\bigg|_{l=0} \Big/ \left(\frac{\partial^2 g(l,0)}{\partial l^2}\bigg|_{l=0}\right)^2. \tag{35}$$

The time dependence of the transverse correlation is then calculated from the energy spectrum $\mathscr{E}(k,\omega)$ (Eq. (25)) from the following relationship (Hinze, 1975):

$$\frac{\partial^2 g(l,\tau)}{\partial l^2} \Big/ \frac{\partial^2 g(l,0)}{\partial l^2} = \frac{1}{2k_0u_0}\frac{\partial^2}{\partial l^2}\int_0^\infty \int_0^\infty \times \left(\frac{\sin(kl)}{kl} - \frac{\sin(kl)}{k^3l^3} + \frac{\cos(kl)}{k^2l^2}\right)\cos(\omega t)\mathscr{E}(k,\omega)\,\mathrm{d}k\,\mathrm{d}w. \tag{36}$$

Integrating and taking the limit as $l \to 0$ results in the following expression for the Eulerian rotational velocity correlation

$$\frac{\langle \dot{\boldsymbol{\Omega}}(0)\dot{\boldsymbol{\Omega}}(\tau)\rangle}{\langle \dot{\boldsymbol{\Omega}}^2\rangle} = \frac{128}{(4+\tau^2w_0^2)^{7/2}} \tag{37}$$

with the integral time calculated as

$$T_\mathrm{r} = \int_0^\infty \frac{128}{(4+\tau^2w_0^2)^{7/2}}\,\mathrm{d}\tau = \frac{16}{15}\frac{1}{w_0}. \tag{38}$$

This analysis provides an estimate of the shape and the magnitude of the Eulerian angular velocity correlation of the fibres. Although derived for short fibre rotation, it is expected that the Eulerian statistics are valid in the limit of long fibres that do not significantly rotate during the integral time scale, T_r, thus provides an upper bound on the Lagrangian integral time scale. However, it is reasonable to assume that the form of the Lagrangian statistics for all fibre lengths can be described by Eq. (37).

The Lagrangian angular velocity correlation of the fibres was calculated and shown in Fig. 12. This figure shows that Eq. (37) provides a reasonable estimate of the form and magnitude in the limit as fibre length increases. The integral time scale was calculated by fitting Eq. (37) to the velocity correlation calculated from the simulation and using the best-fit value of ω_0 and Eq. (38). It was found that for short fibres $T_\mathrm{r} \approx 0.71/(u_0k_0)$ and in the limit of long fibres $T_\mathrm{r} \approx 2.6/(u_0k_0)$.

The long-time rotational dispersion coefficient can now be calculated from the analytical estimate, Eq. (31), by setting $T_\mathrm{r} \approx 0.71/(u_0k_0)$ and assuming it remains constant. Eq. (31) is then plotted and compared with the calculated values of D_r^∞ from the simulation. Fig. 11 shows that the analytical estimate of D_r^∞ underestimates the calculated values. As with the translational dispersion, the underestimate is due to the assumption of a constant T_r.

The integral time scale T_r of the fibre velocity was calculated for all fibre lengths using the best-fit value of ω_0 and Eq. (38) and plotted in Fig. 13. From this figure it is evident that the integral

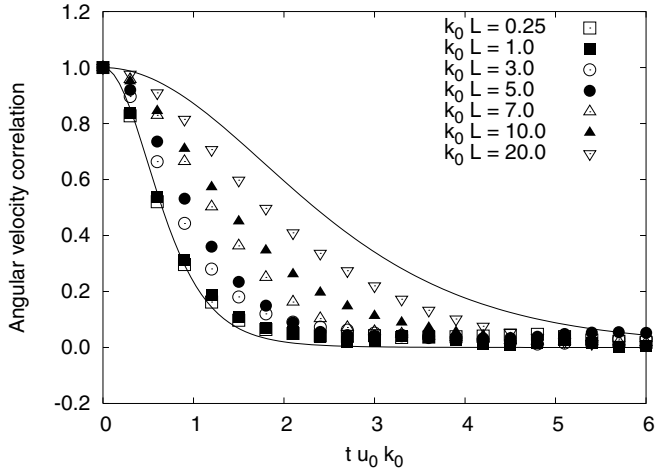

Fig. 12. The Lagrangian angular velocity correlation. Solid lines are Eq. (37).

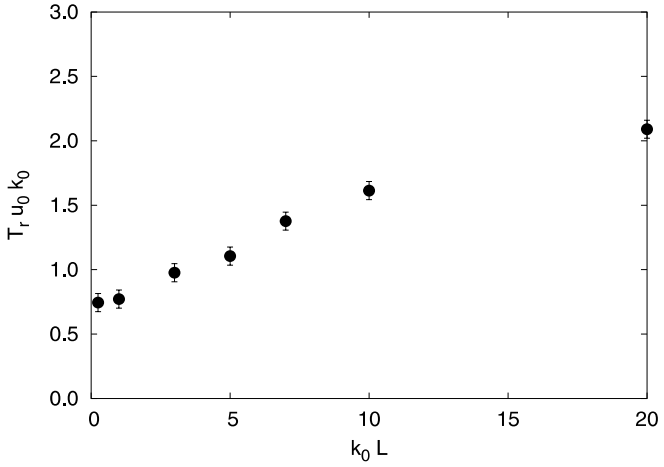

Fig. 13. The fibre's Lagrangian angular velocity integral time scale.

time scale increases significantly with fibre length, from the fluid's Lagrangian correlation for short fibres to the fluid's Eulerian correlation for long fibres. This effect must be taken into account if the effect of fibre length on dispersion is to be accurately modelled.

5. Discussion

In many applications fibre length will be small with respect to the turbulent length scales, i.e. for $L \ll k_0^{-1}$. For this case the long-time, dispersion coefficients are simply given as

$$D_t^{\infty} \approx u_0^2 T_t \tag{39}$$

corresponding to Taylor dispersion of a passive scalar, and

$$D_{\mathrm{r}}^{\infty} \approx \frac{\langle \dot{\boldsymbol{p}}^2 \rangle}{2} T_{\mathrm{r}} = 2\frac{u_0^2}{\lambda_g^2} T_{\mathrm{r}} = \frac{u_0^2 k_0^2}{2} T_{\mathrm{r}}. \tag{40}$$

From the numerical simulation, the Lagrangian integral time scales of the short fibres was determined to be

$$T_{\mathrm{t}} \approx \frac{1.3}{u_0 k_0}, \tag{41}$$

and

$$T_{\mathrm{r}} \approx \frac{0.7}{u_0 k_0}. \tag{42}$$

The value of rotational time scale was significantly smaller than the translational time scale, with $T_{\mathrm{r}}/T_{\mathrm{t}} \approx 0.5$, while the Eulerian analysis of the time scale, valid only in the limit as $L \to \infty$, suggests that

$$\frac{T_{\mathrm{r}}}{T_{\mathrm{t}}} = \frac{4}{5}. \tag{43}$$

The ratio of short-fibre integral time scales estimated from the Eulerian analysis is nearly twice that estimated from the numerical simulation.

The application of this dispersive model of fibre suspensions to computational fluid dynamics requires that the two parameters defining the dispersion coefficients be related to the turbulence model used. If this dispersive model of fibre suspension is to be implemented into a standard κ–ϵ turbulence model, then it is relatively straight forward to show that for short fibres

$$D_{\mathrm{t}}^{\infty} \approx 1.3\left(\frac{5\kappa^2 \nu}{3\epsilon}\right)^{1/2} \tag{44}$$

and the length scale is approximated by

$$D_{\mathrm{r}}^{\infty} \approx 0.7\left(\frac{4\epsilon}{15\nu}\right)^{1/2}, \tag{45}$$

where ν is the kinematic viscosity, $\kappa = 3/2u_0^2$ is the turbulent kinetic energy and $\epsilon = 15\nu u_0^2/\lambda_g^2$ is the dissipation rate. Of course, the analysis presented in this paper is strictly valid only for turbulence with energy spectra well represented by the Kraichnan energy spectrum. Higher energy turbulence needs to consider more appropriate energy spectra.

Before being applied to computational fluid dynamic simulations for designing pulp and paper process equipment, this model needs to be experimentally validated. Future studies will examine the rotational and translational dispersion of fibres in grid-generated turbulence and in wall-bounded shear flow. It is the aim of these studies to directly measure the dispersion coefficients as a function of fibre length. Furthermore, to more accurately model real fibre suspensions the model needs to be extended to include the interaction of fibre orientation and concentration on the turbulent fluid, i.e., provide two-way coupling between the fibres and the fluid, account for an-

isotropic turbulence and provide boundary conditions appropriate for fibre interactions with solid boundaries. These problems are to be addressed in future studies.

6. Conclusion

A numerical simulation of ideal fibres moving in a stochastic model of a turbulent fluid was developed to study the effect of fibre length on dispersion. The results of the simulation were shown to have similar form and magnitude as the analytical estimates provided by Olson and Kerekes (1998). However, the simulation showed that the Lagrangian integral time scale for rotation was significantly smaller than for translation and that the ratio of rotational to translational Lagrangian time scales was smaller than the ratio of Eulerian time scales. The simulation also showed that as fibre length increased the analytic estimates of dispersion under predicted the simulation results and this was due to an increase in the Lagrangian temporal correlation. Furthermore, it was shown that the temporal correlations approached the analytical estimates of the Eulerian correlations in the limit as fibre length increased.

Acknowledgements

This project was funded by the Natural Sciences and Engineering Research Council of Canada and Forest Renewal British Columbia through the Advanced Papermaking Initiative.

Appendix A. Generalized mean fibre dispersion

From Eq. (1), a more general expression for the fibre orientation correlation can be derived. From Eq. (1), the fibre orientation distribution in isotropic turbulence with no mean shear is governed by

$$\frac{\partial \Psi}{\partial t} = D_r \nabla_r^2 \Psi. \tag{A.1}$$

The conditional probability of a fibre having orientation $\boldsymbol{p}$, given that it was in orientation $\boldsymbol{p}_0$ at time $t = 0$, corresponds to the particular solution of Eq. (A.1) with initial condition

$$\Psi(\boldsymbol{p}, t = 0) = \delta(\boldsymbol{p} - \boldsymbol{p}_0). \tag{A.2}$$

The solution of Eqs. (A.1) and (A.2) is the fundamental solution, or Green's function, and is denoted by $G(\boldsymbol{p}, \boldsymbol{p}_0, t)$. From this solution, we calculate $\langle \boldsymbol{p}(t) \cdot \boldsymbol{p}(0) \rangle$, which is a measure of the orientation correlation as

$$\langle \boldsymbol{p}(t) \cdot \boldsymbol{p}(0) \rangle = \frac{1}{4\pi} \int \boldsymbol{p}(t) \cdot \boldsymbol{p}(0) G(\boldsymbol{p}, \boldsymbol{p}_0, t) \, \mathrm{d}\boldsymbol{p} \, \mathrm{d}\boldsymbol{p}_0. \tag{A.3}$$

Although, $G(\boldsymbol{p}, \boldsymbol{p}_0, t)$ can be solved analytically (Berne and Pecora, 1976), it is not always necessary. Again, following Doi and Edwards (1988), we solve the above by considering the time derivative of Eq. (A.3), to arrive at a simple ordinary differential equation, i.e.

$$\begin{aligned}\frac{\partial}{\partial t}\langle \boldsymbol{p}(t)\cdot\boldsymbol{p}(0)\rangle &= \frac{1}{4\pi}\int \boldsymbol{p}(t)\cdot\boldsymbol{p}(0)\frac{\partial G(\boldsymbol{p},\boldsymbol{p}_0,t)}{\partial t}\,\mathrm{d}\boldsymbol{p}\,\mathrm{d}\boldsymbol{p}_0\\ &= \frac{D_\mathrm{r}}{4\pi}\int \boldsymbol{p}(t)\cdot\boldsymbol{p}(0)\nabla_\mathrm{r}^2 G(\boldsymbol{p},\boldsymbol{p}_0,t)\,\mathrm{d}\boldsymbol{p}\,\mathrm{d}\boldsymbol{p}_0\\ &= \frac{D_\mathrm{r}}{4\pi}\int \nabla_\mathrm{r}^2(\boldsymbol{p}(t)\cdot\boldsymbol{p}(0))G(\boldsymbol{p},\boldsymbol{p}_0,t)\,\mathrm{d}\boldsymbol{p}\,\mathrm{d}\boldsymbol{p}_0\\ &= \frac{-2D_\mathrm{r}}{4\pi}\int \boldsymbol{p}(t)\cdot\boldsymbol{p}(0)G(\boldsymbol{p},\boldsymbol{p}_0,t)\,\mathrm{d}\boldsymbol{p}\,\mathrm{d}\boldsymbol{p}_0\\ &= -2D_\mathrm{r}\langle \boldsymbol{p}(t)\cdot\boldsymbol{p}(0)\rangle. \end{aligned} \tag{A.4}$$

Assuming a constant dispersion coefficient, the solution of this equation is given by

$$\langle \boldsymbol{p}(t)\cdot\boldsymbol{p}(0)\rangle = \exp(-2D_\mathrm{r}t). \tag{A.5}$$

This solution is general to large orientation dispersion and demonstrates how the fibre orientation correlation decreases exponentially with time. It also shows that fibres with a small orientation dispersion coefficient, i.e., fibres longer than the length scale of the turbulence, disperse slowly.

References

Berne, B., Pecora, R., 1976. Dynamic Light Scattering. Wiley, New York.

Cox, R.G., 1970. The motion of long slender bodies in a viscous fluid. Part 1. General theory. J. Fluid Mech. 44, 791–810.

Doi, M., Chen, D., 1989. Simulation of aggregating colloids in shear flow. J. Chem. Phys. 90, 5271–5279.

Doi, M., Edwards, S.F., 1988. The Theory of Polymer Dynamics. Clarendon Press, Oxford.

Institut National De Recerche Informatique et en Automatique (INRIA), 1999. Scilab Reference Manual.

Fung, J.C.H., 1993. Gravitational settling of particles and bubbles in homogeneous turbulence. J. Geophys. Res. 98, 20287–20297.

Fung, J.C.H., Hunt, J.C.R., Malik, N.A., Perkins, R.J., 1992. Kinematic simulation of homogeneous turbulence by unsteady random Fourier modes. J. Fluid Mech. 236, 281–318.

Gore, R.A., Crowe, C.T., 1989. Effect of particle size on modulating turbulent intensity. Int. J. Multiphase Flow 15, 279–285.

Hinze, J.O., 1975. Turbulence. McGraw-Hill, New York.

Hunt, J.C.R., Buell, J.C., Wray, A.A., 1987. Big whorls carry little whorls. ASA Reports CTR-S87, pp. 77–94.

Kraichnan, R.J., 1970. Diffusion by random fields. Phys. Fluids 13, 22–31.

McLaughlin, 1994. Numerical computation of particles–turbulence interaction. Int. J. Multiphase Flow 20, 211–232.

Mei, R., 1994. Effect of turbulence on the particle settling velocity in the non-linear drag range. Int. J. Multiphase Flow 20, 273–284.

Maxey, M.R., 1987. The gravitational settling of aerosol particles in homogeneous turbulence and random flow fields. J. Fluid Mech. 174, 441–465.

Newson, R.K., Bruce, C.W., 1998. Orientational properties of fibrous aerosols in atmospheric turbulence. J. Aerosol Sci. 29, 773–797.

Olson, J.A., 1996. The effect of fibre length on passage through narrow apertures. Ph.D. Thesis, Department of Chemical Engineering, The University of British Columbia.

Olson, J.A., Kerekes, R.J., 1998. The motion of fibres in turbulent flow. J. Fluid Mech. 377, 47–64.

Pismen, L.M., Nir, A., 1978. On the motion of suspended particles in stationary homogeneous turbulence. J. Fluid Mech. 84, 193–206.

Pittman, J.F.T., Kasiri, N., 1992. The motion of rigid rod-like particles suspended in non-homogeneous flow fields. Int. J. Multiphase Flow 18, 1077–1091.

Reeks, M.W., 1977. On the motion of small particles suspended in an isotropic turbulent fluid. J. Fluid Mech. 83, 529–546.

Riese, J., Spiegelberg, H., Ebeling, K., 1969. Mechanism of screening: dilute suspensions of stiff fibres at normal incidence. Tappi J. 52, 895–903.

Ross, R.F., Klingenberg, D.J., 1997. Dynamic simulation of flexible fibres composed of linked rigid bodies. J. Chem. Phys. 106, 2949–2960.

Shanker, R., Gillespie Jr., J.W., Guceri, S.I., 1991. On the effect of nonhomogeneous flow fields on the orientation distribution and rheology of fibre suspensions. Polym. Eng. Sci. 31, 161–171.

Snyder, W.H., Lumley, J.L., 1971. Some measurements of particle velocity autocorrelation functions in turbulent flow. J. Fluid Mech. 48, 41–71.

Spelt, P.D., Biesheuvel, A., 1997. On the motion of gas bubbles in homogeneous isotropic turbulence. J. Fluid Mech. 336, 221–244.

Tangsaghasaksri, W., 1994. Über die Sortierung von Fasersuspensionen Mittels Geschlitzter Siebe. Ph.D. Thesis, Darmstad.

Wang, L-P., Stock, D.E., 1992. Numerical simulation of heavy particle dispersion–time step and nonlinear drag considerations. J. Fluids Eng., Trans. ASME 114, 100–106.

Wang, L-P., Stock, D.E., 1994. Numerical simulation of heavy particle dispersion–scale ratio and flow decay considerations. J. Fluids Eng., Trans. ASME 116, 154–163.